1

Climate and Climate Models

The global climate system consists of a large number of interacting parts. The material components and their sub-members include the following:

1) the atmosphere and its constituents such as free molecules and radicals of different chemical species, aerosol particles, and clouds;
2) the ocean waters and their members such as floating ice, dissolved species including electrolytes and gases as well as undissolved matter such as of biological origin and dust;
3) the land components with characteristics such as snow and ice cover, permafrost, moisture, topographical features and vegetation with all its ramifications.

The space–time configuration of abstract fields that are used to characterize properties of interest (such as temperature, density, and momentum) attributed to these components and their sub-members vary with time and position and each exhibits its own spectrum of time and length scales. Heat (or more formally, enthalpy) fluxes, moisture, and momentum fluxes pass from one of these material components to another, sometimes through subtle mechanisms. Determination of whether and how these constituent parts combine to establish a statistical equilibrium may seem challenge enough, but the climate dynamicist also seeks to understand how the system responds to time-dependent changes in certain *control parameters* such as the Sun's brightness, or the chemical composition of the atmosphere. Although we have been at it for many decades now, the grand problem is still far too complicated to solve at the desired level of accuracy (no bias) and precision (error variance) even though preliminary engineering-like calculations are being used routinely in scenario/impact studies because policymakers must (should!) make use of even tentative information in their deliberations (IPCC, 2007, 2013).

Serious attempts at quantitative climate theories can be said to have begun in the late 1960s, although some very clever attempts predate that by decades (see Weart, 2008). The theory of global climate is emerging from its infancy but it hardly constitutes a set of principles that can be converted into reliable numerical forecasts of climate decades ahead or that can be unequivocally used in explaining the paleoclimatic record. However, some valuable insights have been gained and many problems can be cast into the form of conceptual frameworks that can be understood. We now have an idea of which of the components are important for solving certain idealized problems, and indeed, in some cases, it appears that the problems can be made comprehensible (but not strictly quantitative) with models employing only a few variables.

Energy Balance Climate Models, First Edition. Gerald R. North and Kwang-Yul Kim.

The field of climate dynamics is vast, embracing virtually every subfield of the geosciences (even "pure" physics, chemistry, and biology) from the quantum mechanics of photons being scattered, absorbed, and emitted by/from atmospheric molecules in radiative transfer processes to the study of proxies such as tree-ring widths and isotopic evidence based on fossilized species deposited and buried long ago in sediments deep below the ocean's floor. The in-depth coverage of these subfields is generally presented in the traditionally separate course offerings of curricula in the geosciences. This book is concerned with the integration of this array of material into a composite picture of the global climate system through simplified phenomenological models. The approach will be to pose and examine some problems that can be solved or analyzed with the classical techniques of mathematical physics. Throughout we attempt to use these analytical methods, but will introduce and use numerical methods and simulations when necessary. However, our main strategy will be to idealize the physical problem in such a way as to render it solvable or at least approachable, then compare or draw analogies either to the real world or to the results of solving a more believable model – hardly a foolproof procedure but likely to be instructive. In short, we hope to get at the heart of some climate problems in such a way that the reader's intuition for the composite system can be developed and more informed approaches can be taken toward the solution of specific problems.

The energy balance climate models (EBCMs) generally deal with an equation or a set of coupled equations whose solution yields a space–time average of the surface temperature field. Unfortunately, the solutions cannot usually describe the temperature field above the boundary layer of the atmosphere except in rare circumstances. This is a severe limitation, leaving us with only partial answers to many questions we would like to pose. On the other hand, we are blessed with many reasons supporting the importance of the surface temperature field:

1) Space–time averages of surface temperature are easily estimated and many instrumental records provide good data, not just contemporarily, but over the last century.
2) Space–time averages of surface temperature data are close to being normally distributed, making them easy to understand and treat. This is not so for precipitation and some other variables. Moreover, the larger the space–time scale, the more information from point sources can be combined into the average, resulting in a reduction in the random measurement errors on the mean estimates.
3) The time series of space–time averages of surface temperature is particularly simple, resulting in applicability of autoregressive behavior of order unity in many cases.
4) Nearly all paleoclimate indicators provide information about the surface temperature, extending the data base that can be used in testing. There are never enough data to check and adjust models, especially complex numerical models. Paleoclimatology can potentially provide more data that can be used to understand climate models.
5) As we will show, the surface temperature is also the easiest variable to model, especially for large area and time averages. It becomes more difficult as the space–time scales in the problem decrease. In this book, we will start with the largest space and time scales and find that there is a natural progression of estimates from the largest to the smallest space–time scales. Moreover, averaging over large scales reduces some errors in models as well as in measurements.
6) Most of the externally applied perturbations to the climate system that are of interest are directed at large spatial and temporal scales. This happens to be the case for the

four best known perturbations: greenhouse gases, volcanic dust veils, anthropogenic aerosols, and solar brightness. It is intuitively appealing (as well as motivated by physics, as we shall see) that the large space–time scale perturbations result primarily in the same large space–time scales of thermal response patterns in the climate system.

7) The study of energy balance models is cheap. This can be a factor when questions are posed from paleoclimatology, for example. Big models are simply too expensive to experiment with in the first trials. With the speed up of modern computers, many paleoclimate problems can be examined with general circulation models (GCMs), but not every one of them.
8) The study of exoplanets has become important in recent years. The habitable zone of a planet's orbital and atmospheric/oceanic dynamical/chemical parameters may fall into the purview of energy balance models.
9) Finally, the surface temperature is important for societal well-being and it is easily grasped, although the idea of large space–time scales is less easily identifiable and appreciated by the average person.

Unfortunately, as soon as we go above the near-surface environment, the mathematical difficulties of solving the climate problem even for the temperature becomes orders of magnitude more difficult. Also, for all its importance, precipitation cannot be solved by simple models because it depends too sensitively on the circulation of the atmosphere (and the ocean).

1.1 Defining Climate

Before proceeding, we must define what we mean by climate. As an illustrative example, we restrict ourselves at first to the global average surface temperature. Our definition is abstract and not strictly an operational one unless certain (reasonable but, unfortunately, unverifiable) conditions are fulfilled. When we examine records of globally averaged temperature at the Earth's surface we find that it fluctuates in time. Figure 1.1 shows a century-long record of both annual and global averages (*estimates* of these, to be more precise) and, except for a possible upward slope, we find departures from the mean linear trend that persist over a few years or even decades.

Consider an abstraction of the real system. We borrow from the discipline of time series analysis (which may have originated in the subdiscipline of theoretical physics called *statistical mechanics*) the concept of an *ensemble*.[1] By this, we mean to consider a segment of a record of some quantity versus time (e.g., the record of estimates of annual-mean and global-average temperatures in Figure 1.1) as a single *realization* drawn from an infinite number of statistically equivalent (imagined or hypothetical) manifestations of the record. It is presumed that all the realizations are generated from the same physical process (imagine a large number of Earths rattling along but each with slightly different initial conditions set long before the beginning of our "observation" record) for temperature distribution, winds, and so on, but otherwise all the externally imposed conditions such as the Sun's brightness and atmospheric composition are the

1 Ensemble: a group of items viewed as a whole rather than individually.

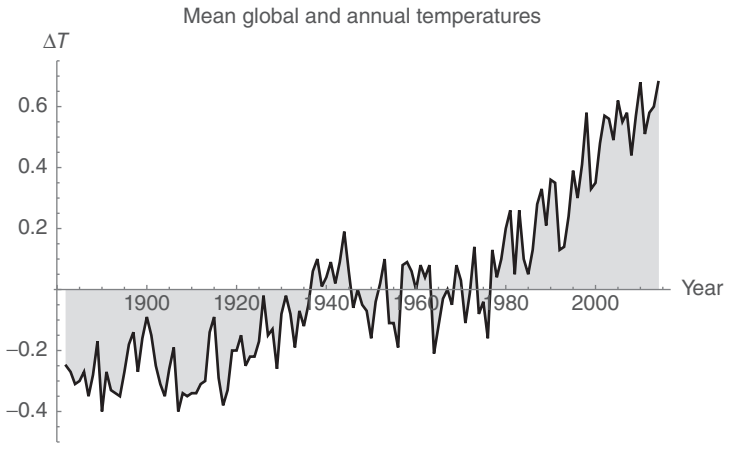

Figure 1.1 Time series of thermometer-based global average temperatures from the website of Goddard Institute for Space Studies: www.giss.nasa.gov. The units are in Kelvin and the temperature values are "anomalies" or deviations from a long-term mean (1951–1980). (Goddard Institute for Space Studies (NASA) (2017).)

same for all the "toy" Earths). The construction of an ensemble is strictly a mathematical convenience, as it allows for ease of computation of moments of the statistical distributions. It is our belief that the realizations form time series that are stationary (defined more precisely below) and that long-term averages of quantities are equivalent to averages across the ensemble members. The advantage of this scheme is that the ensemble provides us with a framework that makes thinking about the problem easier and it facilitates computation of statistical quantities. Also, from a practical point of view this is exactly the way we generate the model climate from a series of simulations from a big climate model (GCM).

The idea of studying a fluctuating system by examining the statistics of individual realizations is called the *frequentist* approach. One can perform statistical tests similarly by asking the probability of occurrence of an event by looking at many realizations of the process. In this book, we will assume the frequentist method is sufficient.

To illustrate the idea, consider a climate that is characterized by a single variable, its temperature[2] $T(t)$. The ensemble average of the temperature at time t is

$$\langle T(t)\rangle \equiv \lim_{N\to\infty} \frac{1}{N} \sum_{i=1}^{N} T^{(i)}(t), \tag{1.1}$$

where the superscript i is an index labeling the ith realization. We imagine calling upon some kind of algorithm that generates realizations for us on command. In the following, we will see how this can be done in a simplified statistical model driven by uncorrelated random numbers. The ensemble of realizations is to have the same statistics (moments) as the real process. We then average over a large number (N) of these to form $\langle T(t)\rangle$. The brackets are defined by the above averaging operation $\langle\cdot\rangle$ (taken in the limit of $N \to \infty$,

2 As always in this book, unless otherwise indicated, we refer to the air temperature a few meters above the land surface, ground or over water, the temperature of the surface level water itself. We will normally use units of Kelvin, but occasionally we will use °C.

but practical experience with GCM simulations suggests that 5–10 is enough for many purposes).

Often in geophysical problems, a long-term temporal mean is equivalent to the ensemble mean:

$$\langle T(t)\rangle \approx \lim_{T_A\to\infty} \frac{1}{T_A}\int_{t-T_A/2}^{t+T_A/2} T^{(i)}(t')\,\mathrm{d}t'. \tag{1.2}$$

A relation like this holds for so-called *ergodic* systems. Roughly speaking, an ergodic system is one for which the physical timescales are bounded (more precision on this shortly). Now that we have the concept of ensemble averaging in mind, we can compute the second moment of $T(t)$:

$$\langle T(t)^2\rangle \equiv \lim_{N\to\infty} \frac{1}{N}\sum_{i=1}^{N} (T^{(i)}(t))^2. \tag{1.3}$$

We could also define the probability density function (*pdf*) of the temperature at time t as $p(T(t))$. We would have

$$\langle T(t)^2\rangle \equiv \int_{-\infty}^{\infty} T(t)^2 p(T(t))\,\mathrm{d}T(t), \tag{1.4}$$

and, for the nth moment,

$$\langle T(t)^n\rangle \equiv \int_{-\infty}^{\infty} T(t)^n p(T(t))\,\mathrm{d}T(t). \tag{1.5}$$

The *variance* is a *centered moment*

$$\mathrm{var}\ T = \sigma_T^2 = \langle (T - \langle T\rangle)^2\rangle. \tag{1.6}$$

We can also consider the *covariance* between the temperature at time t and at another time t'. This is defined as

$$\mathrm{covar}(T(t), T(t')) = \langle (T(t) - \langle T(t)\rangle)(T(t') - \langle T(t')\rangle)\rangle. \tag{1.7}$$

We can think of a *bivariate pdf*, $p(T(t), T(t'))$, in this case. A time series is said to be *stationary* if the mean and variance are independent of t and if $\mathrm{covar}(T(t), T(t'))$ depends only on the time difference $|t - t'|$. These statements mean effectively that there is no preferred origin along the t-axis (at least up to the second moments). In this case, we can write

$$\mathrm{covar}(T(t), T(t')) = \sigma_T^2 \rho(\tau), \tag{1.8}$$

where $\rho(\tau)$ is called the *lagged autocorrelation function*[3] at lag $\tau \equiv |t - t'|$. Note that, by this definition, $\rho(0) = 1$ and $\rho(\tau) = \rho(-\tau)$. Figure 1.2 shows the lagged autocorrelation function for the data in Figure 1.1 (actually, it is the autocorrelation function of the residuals after detrending the data from Figure 1.1 with a straight regression line). The *autocorrelation time* is the integral of $\rho(\tau)$ over all lags (≈ 3.5 years).

$$\mathcal{T} \equiv \int_0^{\infty} \rho(\tau)\,\mathrm{d}\tau. \tag{1.9}$$

3 Strictly speaking, this is called *wide-sense stationarity* because it only considers moments of up to the second order. If the time series elements are normally distributed, this is enough.

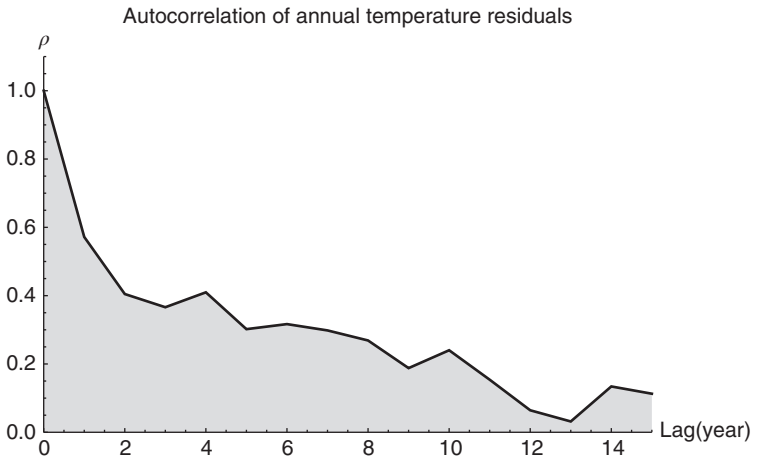

Figure 1.2 Autocorrelation function for the residuals about a linear regression line of the GISS global average surface temperatures. The abscissa is in lagged years. The decay of the autocorrelation indicates the lack of correlation over time. In this case, the autocorrelation function falls to 1/e in about 3.5 years. (Goddard Institute for Space Studies (NASA) (2017).)

Later, we will see how simple models of the system can reproduce curves very similar to that in Figure 1.1 with the added possibility of interpretation of the underlying processes. Here we can get a better idea of what an ergodic system is: the autocorrelation time should be finite. From a practical point of view, it must be short compared to the total length of the time series under consideration.

Instead of real data, we can also generate a time series that resembles a real climate variable. This illustration based on a simple time series algorithm should help in understanding the meaning of some of the above definitions. Figure 1.3 shows five realizations of a time series generated from the *stochastic process* defined by

$$T_n = \lambda T_{n-1} + \gamma Z_{n-1}, \tag{1.10}$$

where T_n is the temperature at time n, a discrete time index (such as an annual average temperature), and Z_n is a random number (variate) that at each time (drawing or *innovation*) takes on a value from a normal distribution with mean zero and standard deviation unity (statisticians indicate this by $Z_n \sim N(0, 1)$); each drawing is statistically independent of the previous one. The constants λ and γ have values (arbitrarily chosen here for cosmetic purposes) 0.8 and 0.05, respectively. In Figure 1.3, the heavy line is the average across the five realizations. If there were a large number of realizations in this process, we would find the average approaching the x-axis (i.e., $\langle T_n \rangle_N \to 0$ as $N \to$ Large). More formally, the standard deviation of the individual points along the heavy curve approaches zero as $\sigma_T/\sqrt{N}$, where σ_T is the standard deviation of the variate T_n, and N is the number of realizations in the ensemble. The process (1.10) that relates the nth value of T_n as proportional to the $(n-1)$th plus a random normally distributed disturbance is called an *autoregressive process of order one* or *AR1*. This particular type of stochastic process is common in geophysical processes such as temperature field evolution. Higher-order autoregressive processes give weights to more distant values in the

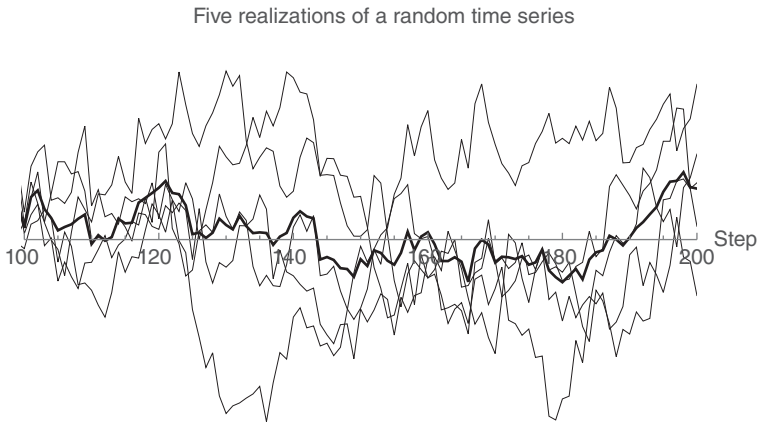

Figure 1.3 Five realizations from a time series generated from the AR1 algorithm $T_n = 0.8T_{n-1} + 0.05Z_{n-1}$, where T_n is a "model temperature" at the nth time step, and Z_n is a random number taken from a normal distribution with mean zero and standard deviation unity. The heavy line is the ensemble average across the five realizations. In this example, the realizations are started at $n = 1$ with $T_1 = 0$. The values from $n = 100$ to 200 are shown. The graphic shows how averaging over only five realizations smooths the time series, diminishing excursions from the mean (=0 here). An observed temperature time series is similar to a single realization.

past than just the last one. Although we will deal with a number of stochastic models in this book, we will find it unnecessary to go beyond the first-order autoregressive process.

We now understand what is meant by a stationary *univariate* climate. By *climate change*, we mean that some moment, typically, the ensemble mean, is subject to a temporal or secular change. For example, the time series in Figure 1.1 appears to have a secular drift upward of about 0.6–0.8 K per century, and over the last half of the twentieth century, even steeper. Another possibility is that the system might experience a step function shift in *forcing*, leading to a climate change from one statistical steady state to a different one after a suitable waiting period (more on this idea in later chapters). As we will see later, the term *forcing* implies an externally imposed imbalance of the planetary energy budget. Such forcings might be time dependent, for example, linear secular increase, abrupt increase (step function), and pulse (delta function).

1.2 Elementary Climate System Anatomy

The vertical structure of the Earth's atmosphere divides nicely into layers each having distinct properties. The layers are conveniently separated according to the slope of temperature profile with respect to the altitude. The *troposphere* lies between the surface and the *tropopause* which in the US Standard Atmosphere is at about 10 km, see Figure 1.4. The layer between 10 km and about 32 km is called the *lower stratosphere* and the part between 32 km and the next slope discontinuity above is the *stratosphere*, which is bounded above by the *stratopause*. In this book, we will confine our attention mainly to the troposphere.

The air above the ground flows with horizontal scales ranging from roughly 1000 km to even larger scales. As it rubs against the surface, turbulence occurs, resulting in a

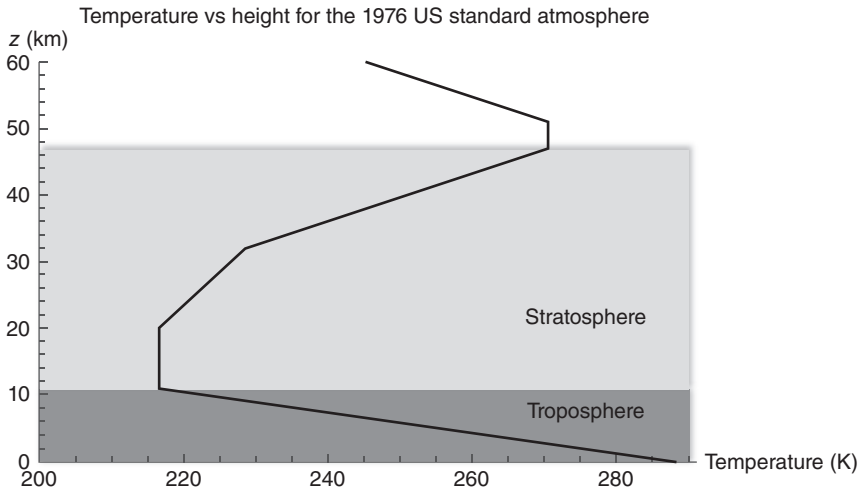

Figure 1.4 The US Standard Atmospheric Profile (solid line). The tropopause is the altitude of the temperature slope discontinuity at 10 km on this graph. The US Standard Atmosphere is an average around the globe. The level of the tropopause here is characteristic of the mid-latitudes. In the tropics, it lies at about 18 km.

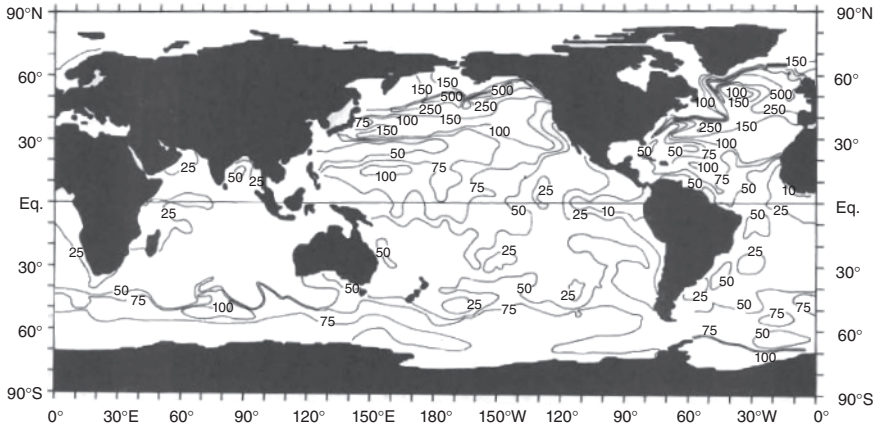

Figure 1.5 March mixed-layer depths (meters) based on a temperature criterion of 0.5 ° C (difference from the temperature at the surface). The ocean's upper layer is well mixed by the action of wind stirring the water. The mixed-layer depth varies by location. It tends to be deeper at higher latitudes and shallow in the tropics. (Taken from Levitus (1982): NOAA Professional Paper, Figure 95a.)

boundary layer near the surface of depth 1–2 km, consisting of well-mixed air. At night, the boundary layer shrinks to a fraction of its daytime depth; then, as the Sun rises, it swells back to its maximum depth of 1–2 km, depending on season and location (see Figure 1.5).

The ocean is complicated, but for our simple-model considerations we will take the top 50 m (sometimes up to 100 m) to be the wind-driven mixed layer that is expected to be vertically homogenized over a period of days (see Figure 1.6) and note the tendency

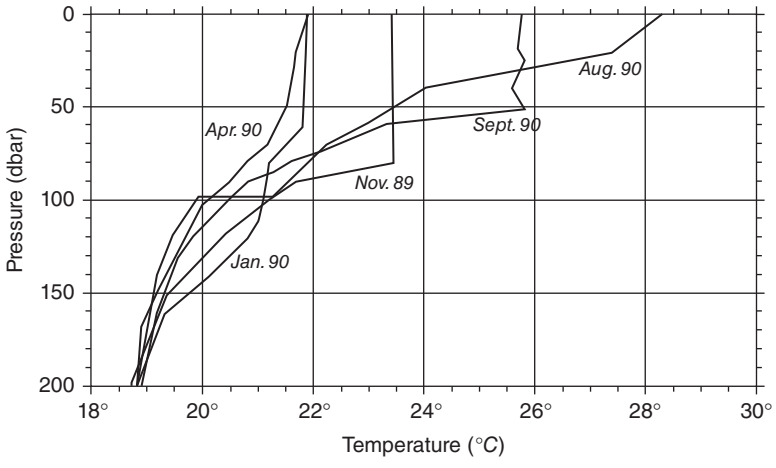

Figure 1.6 Growth and decay of the *mixed layer* and seasonal *thermocline* from November 1989 to September 1990 at the Bermuda Atlantic Time-series Station (bats) at 31.8°N 64.1°W. Data were collected by the Bermuda Biological Station for Research, Inc. Note that pressure in decibars is nearly the same as depth in meters. (Reproduced with kind permission of Robert Stewart.)

for shallow, mixed layers in the tropics and deeper ones in the higher latitudes. The temperature of the ocean is then nearly constant in that upper layer. The temperature falls off from the bottom of the mixed layer to its value (usually around 4 °C, the temperature at which sea water has its maximum density) at very deep levels (approximately several kilometers) approximately exponentially. The e-folding depth of the temperature profile is called the *thermocline*, typically around 500–800 m, depending on season and location (Figure 1.6). The ocean below the mixed layer becomes important when time-dependent perturbations are imposed on timescales longer than a few years. We consider that problem in Chapter 10.

1.3 Radiation and Climate

1.3.1 Solar Radiation

The climate of the Earth is ultimately controlled by the energy output of the Sun and the Earth's orbital elements (see Figure 1.7 for calculations of past values or impacts of the orbital elements, based on Berger, 1978b):

1) The mean annual Earth–Sun distance, currently 149 597 870 700 m. This defines 1 astronomical unit (AU) in planetary astronomy.
2) The eccentricity of the orbit, presently 0.0167 varying between nearly circular value of 0.005 up to 0.06 with a period of roughly 100 ky. See Figure 1.7, which is based on calculations by Berger (1978b). There is little or no effect of eccentricity on the annual, global mean because of Kepler's second law of equal areas of the orbital sweep being equal for equal time intervals. In other words, when the orbiting Earth is closest to the Sun, it is moving faster around its cycle than when it is near aphelion.

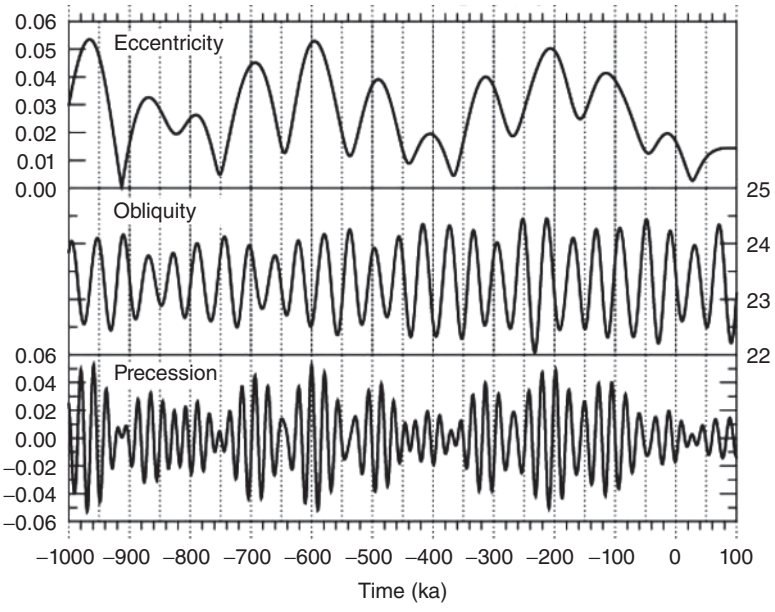

Figure 1.7 The temporal variations of the orbital elements. Upper: Eccentricity (dimensionless); the present value is 0.016. Middle: Obliquity (°) is the tilt angle of the Earth's spin axis from a perpendicular to the orbital plane (the *ecliptic plane*); the present value of the obliquity is 23.5°. Lower: Precession (solar radiation flux density at 65°N in W m^{-2}). This latter shows the variation of this radiation flux density at a latitude thought to be important in forming an ice sheet in North America. (Berger (1978b). © American Meteorological Society. Used with permission.)

3) The angle of the spin axis to a perpendicular to the plain of the orbit, called the *obliquity*, which varies from its present value of 23.5° to between 22.1° and 24.5°. The obliquity varies roughly sinusoidally with a period of about 41 ky. Larger obliquity leads to a larger swing of the seasonal surface temperatures. Zero obliquity leads to a perpetual equinox. Obliquity also has a small influence on the annual mean insolation; large obliquity leads to a slight warming of the annual mean with a north–south symmetrical, hemispherical minimum in lower latitudes.
4) The seasonal phase of *perihelion*, which is the point or calendar time of year on the orbit closest to the Sun along the Earth's elliptical path. The time of equinox shifts slowly through the calendar year owing to two effects: the precession of the spin axis like a top, with period about 26 ky (today the star Polaris sits above the North Pole, but it moves from that position over time, and this has been documented from comparing with ancient astronomers). The equinoxes also precess because of an actual rotation of the major axis of the elliptical figure around the Sun. The two effects cause the calendar date of perihelion to cycle over a 22 ky period. Today, perihelion occurs on December 21, but 11 ky ago it occurred on June 21. The result is a 6% difference in summertime *insolation*[4] at latitude 65°N between summers today and those 11 ky ago. Northern Hemisphere summers would have been warmer (and winters cooler) over continental interiors back then.

4 Insolation is the amount of radiation flux per unit surface area impinging on the Earth at a particular latitude and time of year. Units: W m^{-2}.

5) The chemical composition of the atmosphere. As is by now well accepted, the amount of CO_2 and other greenhouse gases in the atmosphere controls the mean annual temperature of the planet, whereas the aforementioned three effects tend mostly to control the seasonality and/or the latitudinal distribution of the insolation. The changes in CO_2 over the last 800 ky are correlated strongly with the time series of temperatures in Antarctica (Lüthi *et al.*, 2008).

The Sun's luminosity affects the global climate system through the so-called *total solar irradiance* or *TSI* (the amount of radiant energy passing through a unit area perpendicular to the line joining the Earth and the Sun averaged through the year to eliminate the small (∼3%) variation of the Earth–Sun distance due to its slightly elliptical orbit). A number of artificial satellites have been launched over the last four decades for delivering estimates of the TSI. Techniques for analyzing these data have now been perfected sufficiently to provide unbiased estimates of the TSI's average value and its variability for the purposes of climate research. Figure 1.8 shows a graph of measurements from a combination of radiometers aboard a sequence of satellites since the mid-1970s. Much of the high-frequency part of the variation can be attributed to the passage of sunspots across the face of the Sun as it rotates with a period of about 25 days. The longer term trends are consistent with a weak quasi-periodicity of 11 years commensurate with the solar cycle of the frequency (number per year) of appearance of sunspots. The amplitude of the oscillation (at least over the few cycles observed during the *satellite era*) is about 0.1%. The most modern estimate of the absolute magnitude of the TSI is $\sigma_\odot \approx 1360.45 \mathrm{W\,m^{-2}}$. This value is somewhat smaller than the average shown in Figure 1.8 as the value quoted here is based on a recent highly reliable calibration (Kopp and Lean, 2011; Coddington *et al.*, 2016[5]). It is not yet clear whether the Sun's output varies on longer time scales.

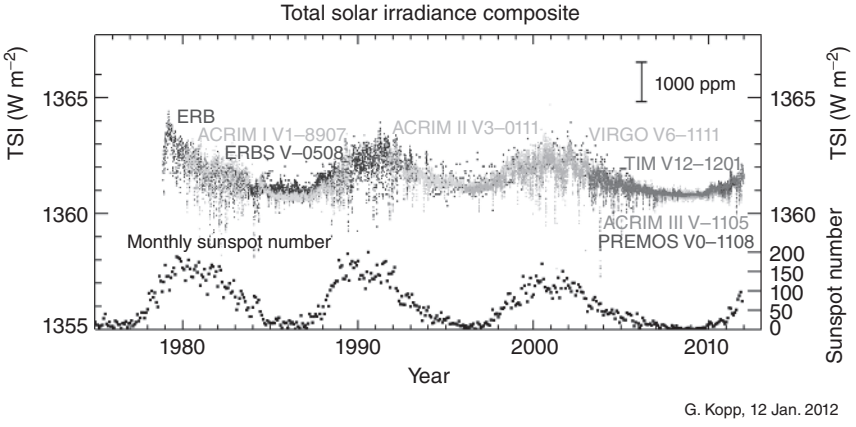

Figure 1.8 Time series of the TSI (total solar irradiance) over the last three solar cycles. The TSI is the radiation energy flux density (in $\mathrm{W\,m^{-2}}$) reaching the top of the atmosphere. It is averaged through the year as the Earth passes around its elliptical orbit. The upper curve (points) are newly calibrated and reconciled data for the TSI from a variety of instruments over the satellite era ($\mathrm{W\,m^{-2}}$). The lower curve is the monthly count of sunspots. (Reproduced with kind permission of Kopp (2017).)

5 Coddington *et al.* (2016) present explanations and graphics clarifying how the sunspots and facula (bright zones around the dark sunspots) compete in modulating the TSI.

A longstanding conjecture is that the Sun was less bright during the *Maunder Minimum*, a period of about a century starting in 1650 AD, in which there were essentially no sunspots (Eddy, 1976). So far no compelling evidence for the validity of this attractive conjecture has been published. Over ultralong time scales it is strongly suggested by astrophysical theory that the solar constant should have steadily increased by about 30% over the last 4.7×10^9 years, Gough (1981).

The Sun radiates approximately as a blackbody whose temperature is about 5770 K over most of the emission spectrum as seen in Figure 1.9. The distribution of the radiation by wavelength is important in determining how much of the radiation penetrates to various depths in the atmosphere before being absorbed or scattered. Very short wavelength radiation (X-rays, extreme UV, etc.) are absorbed in the upper atmosphere, while UV of shorter wavelength than 273 nm (nm = nanometers) is absorbed by ozone (O_3) in the stratosphere (Pierrehumbert, 2011).

Figure 1.9 (modified from Gray *et al.*, 2010) shows the distribution of solar flux as a function of wavelength. Most of the radiation power is in the visible part of the spectrum, but a large part is also in the near infrared ($\lambda > 800$ nm $= 800 \times 10^{-9}$ m). Disposition of the solar radiation entering the top of the atmosphere is as follows: 23% is reflected back to space by clouds and particles suspended in the air, 4% is reflected back to space by the

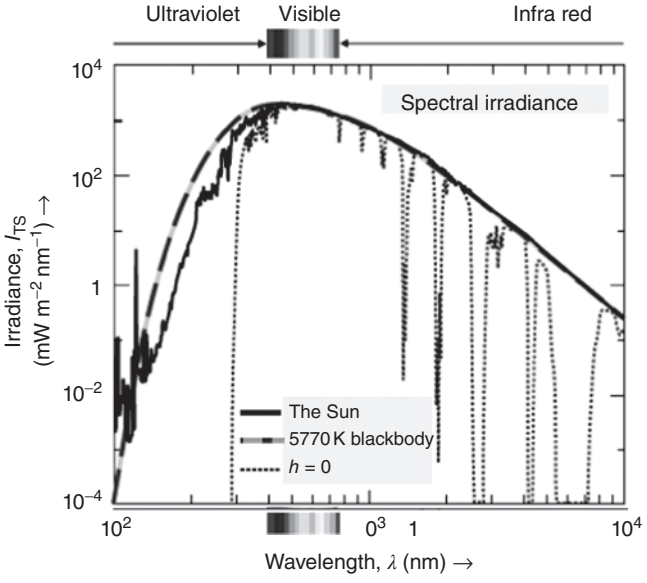

Figure 1.9 Spectral irradiance from the Sun (black line). Spectral irradiance means the Sun's rays are decomposed into wavelengths in order to reveal how different wavelength bands are disposed of by the Earth's atmosphere. The black and gray long-dashed smooth curve is the distribution of incoming radiation from an imaginary black body whose temperature is 5770 K, which is a rather good model for the Sun's radiation. The solid black curve indicates the actual radiation from the Sun. It differs some from the blackbody especially in the ultraviolet and shorter wavelengths. The dotted lines indicate the absorption of sunlight as a function of wavelength by the clear atmosphere as seen from the ground ($h = 0$). The attenuation is cut off by atmospheric gases for wavelengths below about 270 nm. Other absorption due to molecular interactions occurs in the infrared. (Gray *et al.* (2010). Reproduced with permission of American Geophysical Union.)

surface; 23% is absorbed by water vapor, clouds, dust, and ozone, and 47% is absorbed at the surface. About 30% of the total is reflected back to space (planetary albedo) and the rest goes into heating the system. Recent research suggests that the UV radiation varies appreciably more over the 11-year cycle than the TSI and that this variation can lead to a faint 11-year cycle in some climate variables (Haigh, 2010).

Figure 1.9 shows the total column absorption by the atmosphere as a function of wavelength as the gray-dotted line. The spectrum of absorptivity is very complicated to say the least. The interplay between the incoming and outgoing radiation and this spectrum along with the atmosphere's dynamic reaction to it is a key ingredient in determining the vertical structure of the atmospheric column of air at a point at the surface and ultimately in determining the horizontal movements in the system components as well.

1.3.2 Albedo of the Earth–Atmosphere System

The climate system only makes use of the solar radiation that is absorbed by the Earth–atmosphere combination. The unused fraction of the solar radiation flux reflected by the system back to space (referred to as the *planetary albedo*, averaged over the globe, through the diurnal and annual cycles) is governed by a number of factors, several of which are dynamically determined within the system. Artificial satellite-based instruments providing estimates of the albedo of the Earth–atmosphere system have been conducted since the mid-seventies. Trenberth *et al*. (2009, always subject to updates) summarize the current status of the Earth Radiation Budget estimates and the associated errors (see also Loeb *et al.*, 2009; Loeb and Wielicki, 2014). Figure 1.10 shows the flows of energy entering from space in the visible part of the spectrum and its

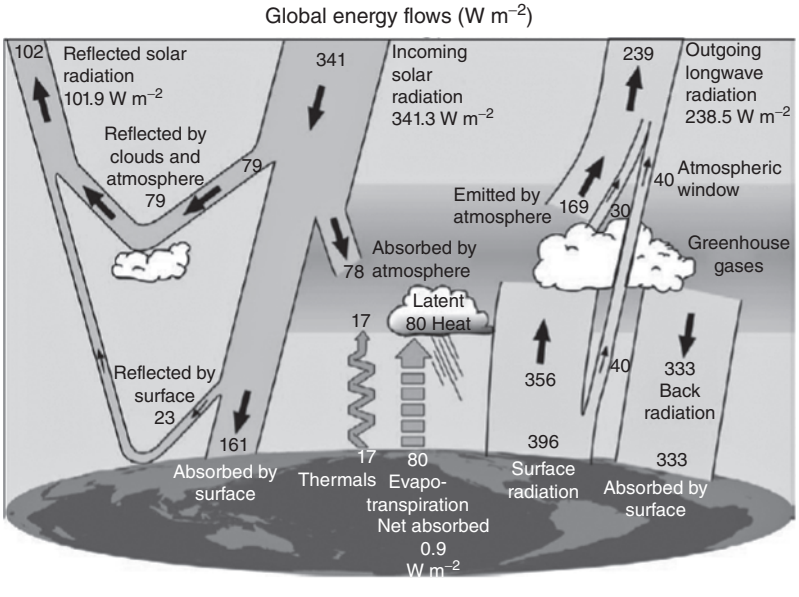

Figure 1.10 Schematic of energy flows in the globally averaged Earth–atmosphere system. Arrows indicate flux densities. The incoming solar flux is divided by 4 to take into account the ratio of the Earth's total area to the area of its silhouette. (Trenberth *et al.* (2009). © American Meteorological Society. Used with permission.)

apportionment into different flows in the Earth–atmosphere system. We can estimate the planetary albedo from the data in the figure ($102/341 \approx 0.30$).

1.3.3 Terrestrial Infrared Radiation into Space (The IR or Longwave Radiation)

Besides measuring the albedo[6] of the planet in small latitude–longitude boxes, satellite observatories also provide estimates of the outgoing infrared radiation fluxes at the top of the atmosphere. These are typically also for month-long averages but over $10° \times 10°$ boxes. It is possible to find a relationship of the outgoing radiation with the surface temperature by a comparison of the two data sets as shown in Figure 1.11. This suggests that, for many rough calculations, the outgoing infrared flux leaving the top of the atmosphere can be approximated by a linear relationship[7] with slope 1.90 W m^{-2} °C^{-1}. Analysis of 10 years of data from the Nimbus 6 and Nimbus 7 satellites in mid-latitudes yields essentially the same relationship as with the Earth Radiation Budget Experiment

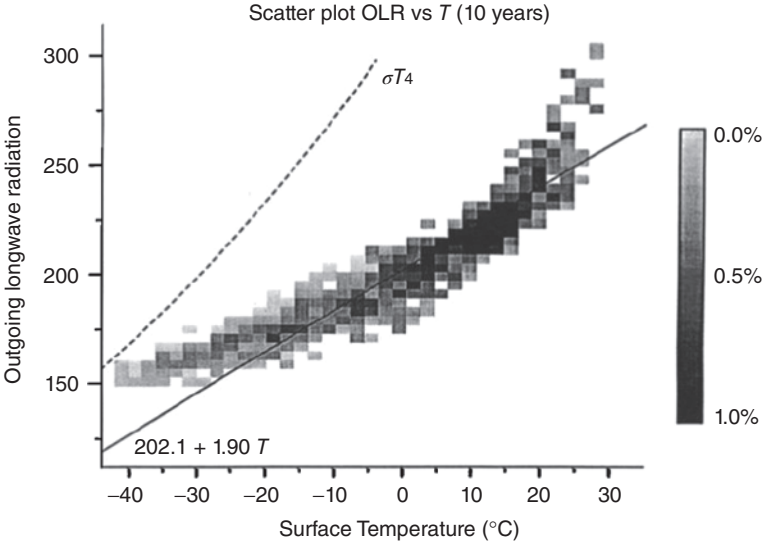

Figure 1.11 Density plot of outgoing infrared radiation flux versus surface temperature taken from satellite data. The radiation data from different locations and seasons against the local month-averaged temperature at the surface for the same actual month when the satellite data were collected. Darker shading indicates greater frequency of occurrence. These data are for the entire sky, that is, cloudy portions are not omitted. Note that the curve and its slope are lower than that of a blackbody curve (dashed curve). The linear radiation law due to Budyko is subject to many shortcomings, but as a tool it has proven useful in energy balance models. (Graves *et al.* (1993). Reproduced with permission of Wiley.)

6 Strictly speaking the satellite-based radiometer measures solar-reflected radiation as a function of the angles involved and these data are converted to values on a grid.

7 The tropical latitudes (not shown here) actually exhibit a negative correlation with local surface temperature because clouds (convection) tend to migrate to the hottest points on the surface. This clustering of clouds at surface hot spots leads to a decrease of outgoing radiation in these regions because the intense convection leads to high cloud tops that are cool and radiate less than a clear area would. In energy balance models, this is somewhat compensated by the fact that the albedo is increased where the clouds are more concentrated.

(ERBE) data (see Graves *et al.*, 1993). Furthermore, the low-frequency filtered part of the terrestrial radiation to space (periods between 1 and 10 years) also yield essentially the same regression slopes. This presumably means that the relationship between IR and surface temperature holds for slow climate changes as well as the faster seasonal cycle (see the intercomparison of GCM results for sensitivity by Cess *et al.*, 1990). It is important to realize that the relationship between outgoing IR and surface temperature is not a result of simple radiative-transfer calculations but is an empirical relationship between the equilibrium ground temperature and the outgoing radiation flux. The atmospheric column undergoes convective overturning adjustments in establishing the relationship (see Chapters 3 and 4). Despite the encouraging results just mentioned, this technique of obtaining the slope of the linear regression line is subject to a variety of errors. For example, the outgoing radiation from latitude to latitude and/or from season to season at a point might be very different from that occurring during a secular change in forcing. Hence, use of the linear infrared radiation rule (attributed to Budyko, 1968; who, having no satellite data, came upon the rule using radiative-transfer calculations) may be very convenient in our calculations, but the strict numerical values are not to be taken literally.

Convective adjustment happens automatically in the atmospheric column because the shape of the atmospheric profile derived without convection is unstable to overturning if the vertical profile of the temperature is determined solely by the radiative heating and cooling (so-called *radiative equilibrium*; see Chapter 3). Incidentally, convective adjustment leads to the global average constant lapse rate of about $6.5\,\mathrm{K\,km^{-1}}$ in the troposphere. Referring to Figure 1.10, if we try to account for the unreflected $239\,\mathrm{W\,m^{-2}}$ fraction of radiation energy out of $341\,\mathrm{W\,m^{-2}}$ initially delivered to the top of the atmosphere (per unit area of the spherical Earth) by the Sun, we find that the energy flux density bifurcates taking a variety of paths through the Earth–atmosphere system before the $239\,\mathrm{W\,m^{-2}}$ is finally returned to space. For example, much of the solar radiation absorbed by the surface ($161\,\mathrm{W\,m^{-2}}$) is released from and cools the surface by *thermals* (or dry convection) and *evapotranspiration*, which includes the flux of water vapor from the biosphere. Both processes deposit the heat energy in sensible form in the atmosphere above, warming it. Huge amounts of energy are radiated from the surface ($396\,\mathrm{W\,m^{-2}}$), most of which is absorbed in the atmosphere and radiated back down as well as upward ($333\,\mathrm{W\,m^{-2}}$), rewarming the surface. The sky actually warms our faces as we stand outside on a hot day. Finally, the heat-induced radiation trickles out the top of the atmosphere to space. The various components thus come to a statistical equilibrium (fluctuating, but statistically stationary in time). For the seasonal cycle, the equilibrium is cyclic and the statistical term for it is *cyclostationary*. For an EBM example of its use, see Kim and North (1997).

1.4 Hierarchy of Climate Models

Climate models fit into a hierarchy[8] that we believe is helpful to understanding the complete system. At the low end of the model hierarchy are the global average planetary

8 One of the earliest and best review papers discussing the hierarchy of climate models is that of Schneider and Dickinson (1974). Isaac Held makes a strong case for a hierarchical approach in Held (2005).

models to be discussed in the next chapter. In these global models, the climate consists of a single variable, the surface temperature. As we will see in the next few chapters, some global average models will include a vertical dependence, so that the climate consists of a single function of altitude. The hierarchy is topped off by the GCMs. Each long run can be considered a detailed *realization* of an artificial climate system including all the weather-scale fluctuations. In keeping with this view, we might consider a string of actual data about the Earth's global average temperature as a single realization taken from an imaginary ensemble of such realizations. The currently most sophisticated system models couple the circulation of the atmosphere with that of the ocean and other components such as the biosphere and the cryosphere (ice parts such as glaciers, sea ice, and permafrost). Part way along are the models that omit the slower components and concentrate on the circulation and thermodynamic indices of the atmosphere. We will have cause to discuss these models frequently, as they provide artificial realizations of the faster part of the climate system and they are especially helpful in understanding the relation of simpler model ideas to the greater system.

1.4.1 General Circulation Models (GCMs)

General Circulation Models (GCMs) have evolved from the numerical weather forecast models of the 1950s. Those short-range forecasting models have stood the test of time day in and day out over this period. The upgrading of numerical methods and the implementation of improved representation of the physical components and mechanisms have led to steady improvement of their forecasting performance and their ability to simulate, with reasonable certainty, the evolution of most middle-latitude storm systems that are so important in transporting heat and other quantities across latitude circles. In addition, much of the variability of the climate system originates in these disturbances.

A short-term weather forecast does not depend much on tiny trends of imbalance in the overall energy balance such as might occur at the top of the atmosphere owing to solar brightness changes or a trend of CO_2 amounting to 0.0014% per day. Not much happens owing to such an imbalance in a day or two. To make a climate simulation model, one has to go back to the fundamentals and include accurate radiative transfer modules in the computer code to take these seemingly tiny effects into account. Over decades, they matter. Today's models still struggle to properly include aerosols and clouds in their radiation budgets. These are known problems. There may very well exist problems we do not yet know about.

Following the pioneering numerical experiment by Phillips (1956) on modeling the atmosphere's general circulation with one of the original digital computers, modeling groups began to respond. The leaders included Kasahara, Washington, Smagorinsky, Manabe, Arakawa, and Leith (see the book by Donner *et al.*, 2011). The first climate models in the 1960s were run at mean annual solar distribution over the planet (no seasons) and a surface that was composed of dry land partially covered with moist surface and an ocean with wet surface. Among many pioneering studies, a particularly influential one was conducted by Manabe and Wetherald (1975). The model included very simple geography (land alternating with ocean at 60° longitude segments). There were no seasons and the ocean was a simple wet surface. The vertical structure consisted of nine layers and the horizontal resolution (grid-box size) was approximately 500 km. Water substance in the atmosphere was computed as vapor and was allowed to evaporate from the surface when conditions were right, and then carried by the simulated

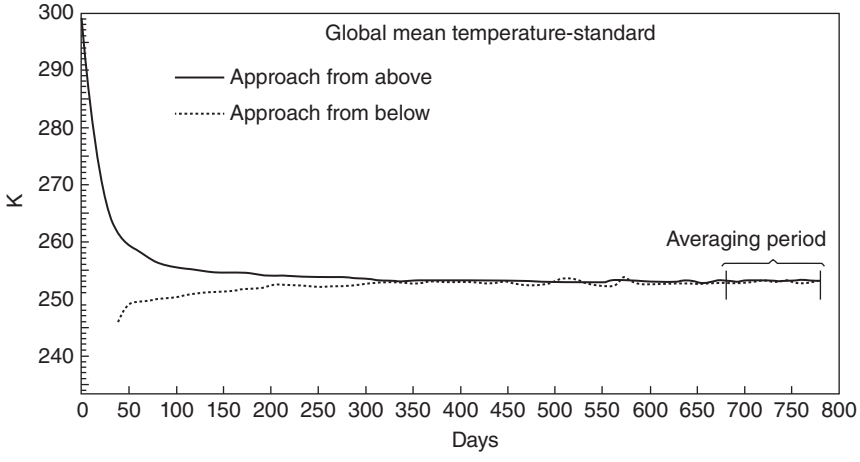

Figure 1.12 Time evolution of two runs from a very early general circulation model (GCM) with different initial conditions (one cold the other warm) by Manabe and Wetherald (1975). The globally averaged (mass-weighted) temperature of the atmosphere in the two runs eventually settles down to approximately the same statistical steady state. (Manabe and Wetherald (1975). © American Meteorological Society. Used with permission.)

winds; the model produced its own precipitation. Relative humidity was computed as fluxes of water into and out of grid boxes as warranted. Interestingly, the relative humidity near the surface remained rather steady through the integrations of climate change. The model was initialized in a cold state and a separate run was made with an initial warm state (Figure 1.12) and both solutions evolved to the same statistical steady state fluctuating endlessly but essentially randomly about a constant mean; that is, it continued to fluctuate but the statistics of the fluctuations formed a stationary time series. Moreover, the latitudinal dependence of the temperature distribution looked qualitatively similar to that of the annual average for the planet Earth. Surely, the authors were pleased with this very remarkable result, and the age of climate simulation was thus launched.

Emboldened, Manabe and Wetherald, and other fledgling GCM groups, proceeded to double the CO_2 in the model atmosphere from 300 to 600 ppm. The resulting globally averaged surface temperature increased by 2.93°, a result eerily close to the value of the most modern simulations nearly 40 years later. The latitudinal and vertical dependences of the temperature change are given in Figure 1.13. Note the cooling in the stratosphere, a finding that still holds in simulations from the most recent high-resolution models. The cooling of the lower stratosphere during CO_2-forced warming at the surface is also a rather simple consideration of energy balances in the vertical layers of the atmosphere that we will discuss in Chapter 4.

1.4.2 Energy Balance Climate Models

This book focuses on the low end of the climate model hierarchy because it is a good entry point for those wanting to learn about climate models, but also because the nomenclature and many concepts introduced at this level apply all the way up the hierarchy. Our primary focus is the class of so-called EBCMs (sometimes they are

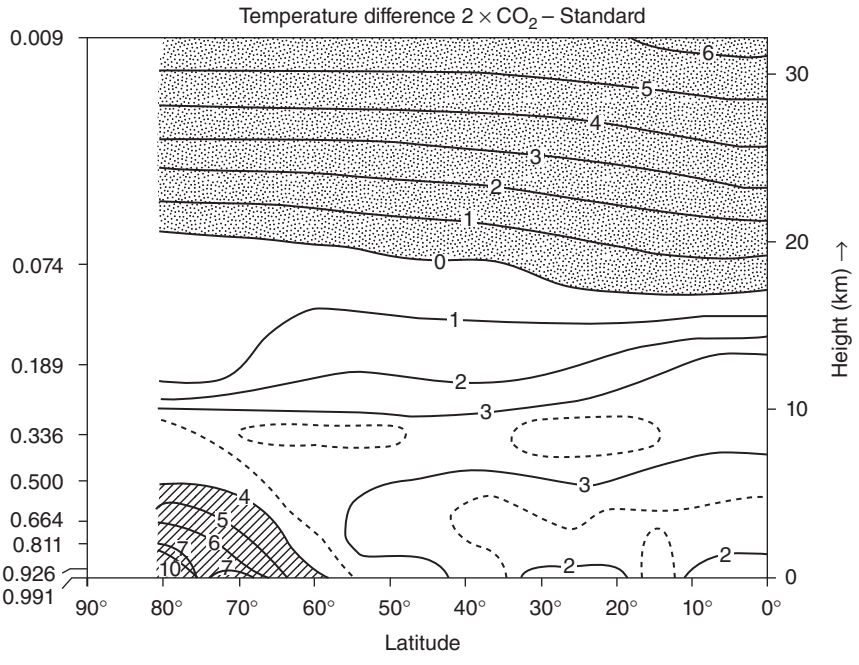

Figure 1.13 Change of temperature (°C) after reaching equilibrium from a change due to doubling CO_2, based on the 1975 GCM (same as in the previous figure). The stippled areas indicate negative changes. Note the appearance of a very interesting phenomenon: the cooling of the lower stratosphere. (Manabe and Wetherald (1975). © American Meteorological Society. Used with permission.)

referred to simply as *energy balance models* or *EBMs*). EBMs were introduced by Budyko (1968) and Sellers (1969) independently and they are often justly referred to as the *Budyko–Sellers* models. There was also an earlier paper by the astrophysicist (Öpik, 1965) that used an EBM with ice cover. Their first papers brought to light the possibility that a modest lowering (a small percentage) of the TSI would lead to an expansion of the polar ice caps from their present area of a about 5% of the Earth's surface area to a complete covering of the planet by an ice sheet. This alarming finding called attention to the potential fragility of the Earth's climate and it sparked the explosion of climate modeling research that followed. At first, the interest was not so much in the effects of increasing CO_2, but with solar brightness changes, the effect of screening of sunlight by volcanic dust veils, and anthropogenic aerosols. Also, there was the possibility of explaining the ice ages.

As GCMs began their remarkable ascent, in parallel, EBMs were subjects of experimentation by many groups and individuals. Held and Suarez (1974) studied the Budyko model and improved on it. Using a method inspired by Chýlek and Coakley (1975), North (1975a; 1975b) solved analytically the latitude-dependent ice cap model similar to the Budyko and Sellers versions but with a constant thermal diffusion coefficient. The stability of the solutions was investigated numerically by Ghil (1976) and Gal-Chen and Schneider (1976); also, analytically by Cahalan and North (1979) and North et al. (1979),

Golitsyn and Mokhov (1978). Many other references can be found in the early review article by North *et al.* (1981).

The essence of the EBMs is their conceptual simplicity, despite some of the rather involved mathematical methods required to solve them. We favor the analytical solution, not only because it is more elegant but also because such methods often lead to a deeper understanding. Often in this book and elsewhere in the literature, some less mathematically inclined readers can grasp the conceptual basis of a model and skip directly to the graphs that capture the solutions, with the comfort that the curves are backed up by an analytical or an uncontroversial straightforward numerical solution. There are many shades to the word "skip" here.

1.4.3 Adjustable Parameters in Phenomenological Models

All EBMs contain empirical parameters such as the slope and intercept of Budyko's infrared radiation rule or the thermal diffusion coefficient in latitudinally dependent models. As more independent variables are included, the number of such empirical coefficients increases. The beauty of the approach is that the model's use of phenomenological coefficients keeps the approach close to the large-scale observations. The downside is that we have departed from first principles, and we cannot know how such a coefficient might change as the climate changes. In the case of GCMs, the analog is the grid resolution: as the grid is made finer, or as more physical processes are included, there is more physical realism, but inevitably more parameters are needed. The values of the coefficients have to be "tuned" to fit what little data there are. It is often instructive to "back off" and view the system with less resolution (in its broadest sense).

With EBMs, there are two approaches:

1) Use as few empirical or phenomenological coefficients as possible to see if the main features of the model are robust. This would be important in early tests of a hypothesis where one is not interested in quantitative results over qualitative features. The advantage of this approach is to keep the number of free parameters as small as possible: the idea of *parsimony*, often discussed in fitting models in the statistical literature.[9] As we proceed in the story, we will try at each stage to tell what value is added (or lost) by the addition of a new phenomenological parameter.
2) One is interested in quantitative results in, for example, the detection of faint signals (such as the response of the surface temperature of the Earth to the solar cycle of brightness). Here one might introduce more than the minimal number of phenomenological parameters in order to establish a base state from which a perturbed solution is required. In this case, one might sacrifice parsimony of the number of freely adjustable coefficients in order to obtain the best value of the perturbed climate as possible within the EBM framework.

Cautionary Note: It is extremely tempting to add to a simple EBM. Do it at extreme risk. Depending on the problem you are addressing, you might be overfitting, that is, adding a new parameter which can be adjusted to get whatever result you wish. Such an addition could "explain" a certain phenomenon, but it is not likely to be unique.

---

9 For example, see p. 223 of Montgomery *et al.* (2001).

1.5 Greenhouse Effect and Modern Climate Change

The greenhouse effect has become a prototype of climate change studies. Solar radiation passes essentially unaltered through the atmosphere to the surface where about half of it is absorbed. Some absorption also occurs in the atmosphere, warming the local surroundings; in the troposphere, convection spreads this heat energy (enthalpy) from its top to its bottom. Heat (enthalpy) leaves the surface as infrared radiation, sensible heat flux (e.g., thermals or dry convection), and latent heat flux (heat that is removed from the surface by evaporation, then released aloft as sensible heat in cloud formation), all heating the troposphere. The heated troposphere radiates toward the surface as well as upward toward outer space. The eventual radiation to space is from colder material than that at the surface, the rate being that corresponding to a 255 K blackbody. The result is a surface temperature some 30 °C above what it would have been for a non-absorbing atmosphere. The ever-lurking question of what happens as the concentrations of certain trace gases such as carbon dioxide and methane increase exponentially over the next century will be discussed in Chapter 4.

1.6 Reading This Book

We expect readers from many disciplines to read or at least peruse this book. The primary audience is likely to be from the climate science community, which covers many subfields from meteorology, oceanography, atmospheric chemistry, paleoclimatology, and other geosciences. But in addition we hope to interest readers from physics, applied mathematics, statistical sciences, economics, and engineering. The models are rich in interesting problems, many remaining unsolved. We have chosen mostly to exploit problems in which standard low-level theoretical physics is employed, but there are forays into stochastic processes and more modern methods. We generally take the method of old-fashioned mathematical physics and some mathematically inclined readers may occasionally shudder at our glossing over mathematical technicalities. We hope our sins of omission lead others to be inspired to clean up after us. In our opinion, the field of climate science could benefit from the entry of mathematically, statistically, and physically talented innovators. As you read these chapters, you should find many intriguing problems to work on.

The following is a summary of the topics with help on what can be skipped on first reading.

- The book really begins in Chapter 2 in which most of the methods of the rest of the book are presented in the context of the model for the globally averaged temperature. In Chapter 2, the mean annual temperature of the planet is determined from the most elementary principles of radiation balance at the top of the atmosphere. We find how the planetary temperature returns to its equilibrium state if perturbed and we proceed to see how it responds to periodic disturbances. We can also see how the variations of planetary climate can be modeled by taking the fluctuating weather as a driving force, tickling the more sluggish response of the temperature field. This allows us to see how a noisy system like climate can be predictable. We will also see how the system responds to external forcings such as imposed imbalances such as changes in the solar brightness or changes in greenhouse gases.

- Chapters 3 and 4 can be skipped by many readers as, to some extent, they are a diversion from Chapter 2 and the later chapters. But they explain in some detail a few idealized models of the vertical structure of the atmosphere (radiative equilibrium and radiative-convective equilibrium in a gray atmosphere), and how that structure changes with perturbations. Chapter 4 gives a detailed look at the spectra of infrared radiation, the heart and soul of the greenhouse effect, without much mathematics. An online calculator is used to compute the effect of doubling CO_2 when no feedback mechanisms are in play. Then a detailed discussion of feedbacks is presented. Both of these chapters stand by themselves. Chapter 4 should interest many readers who might not be interested in other parts of the book, as it purports to show exactly how the rather subtle greenhouse effect actually works.
- Chapter 5 resumes the study of the surface temperature, but now it considers the latitudinal dependence of the surface temperature as modeled by diffusion of thermal energy (macroturbulent heat conduction) across latitude belts. As with Chapter 2, it delves into the aspects of steady-state models. The upshot is a model solution developed into a series of Legendre polynomials whose coefficients are temperature mode amplitudes corresponding to decreasing latitudinal space scales. It is shown that a satisfactory solution involves only the first two Legendre modes, indexed 0 and 2. A derivation of the poleward transport of heat as a function of latitude is provided with a comparison with data.
- Chapter 6 extends the previous chapter to incorporate time dependence, including the seasonal cycle. A derivation of the insolation function is presented, revealing its dependence on the orbital elements: eccentricity, obliquity, and precession. The insolation and model solutions again involve Legendre polynomial modes. Each thermal mode has a characteristic decay time scale. Smaller spatial scales lead to shorter time scales. There is a discussion of a heuristic connection between the random fluctuations of the mid-latitude storm systems and the transport of thermal energy as being diffusive in ensemble average. Also brief attention is given to numerical techniques.
- Chapter 7 introduces the nonlinear ice-cap feedback mechanism and finds an analytical solution to it for the one-dimensional models. The examination reveals multiple solutions for a particular set of external controls (such as solar brightness or CO_2 concentration). The nonlinear ice-cap model is a marvelous example of how bifurcations (in the popular literature: tipping points) can appear in these simple model structures. Mathematicians and theoretical physicists might find ways of extending some of these results.
- Chapter 8 begins a new class of models with two horizontal dimensions. This leap in dimension is achieved by allowing the local heat capacity of the air–land–ocean column to have a position dependence over the planet. The effective heat capacity over ocean (mixed layer) is about two orders of magnitude larger than that over land. Sea ice cover is somewhere in between. The spherical harmonic basis set is introduced to span the globe. With essentially no further changes, the model delivers the seasonal cycle surprisingly accurately over the globe. Because the Earth's land–sea geography is so complex (shorelines), one must resort to numerical solutions on the sphere. Readers with less interest in the mathematical details can read the first few pages and skip to the graphics.
- Chapter 9 extends the previous chapter by introducing white noise forcing to simulate weather fluctuations. Without any new parameters from the previous chapter,

the model shows the geographical dependence of the temperature variance. Moreover, even the correlation lengths and their frequency dependence come out of the solutions. Again, less mathematically inclined readers can read the first pages and skip to the figures.

- Chapter 10 returns to the problem of how the ocean delays and suppresses the response to time-dependent forcings, starting with a single mixed-layer slab. More complicated systems are treated, including slabs below the mixed layer. The problem of the response to periodic forcing at the surface is solved for vertically diffused heat.
- The book ends (Chapters 11 and 12) with a few applications of EBMs. Chapter 11 covers some estimation problems in climate science, such as the uncertainty of estimating global averages of surface temperature drawn from a finite number of dispersed point sources of information and the detection of faint signals in the climate system. In both cases, the EBMs are used to help understand the procedures involved in the estimation processes. In fact, they fare rather well against their bigger cousins.
- Chapter 12 surveys the use of EBMs in the pursuit of solutions of a variety of paleoclimate problems. Paleoclimatologists can see how simple EBMs can be used to treat some of these problems after they peruse the relevant earlier chapters and Chapters 8 and 9. First the faint Sun paradox is considered, then glaciations in deep time (the late Paleozoic) and the initiation of glaciation on Antarctica and Greenland. Finally, progress in understanding the glaciations of the Pleistocene is discussed briefly.

1.7 Cautionary Note and Disclaimer

Everyone reading this book should recognize that climate models are pretty blunt instruments and this especially holds for EBMs. We should think of the EBMs (others, too) as *analogies* to the climate system. They give us insight into the dominant features of this incredibly complex field of interacting components and help guide us to implement better models and/or more-relevant observing systems. It should be no surprise that after 40 years of this endeavor, the sensitivity to climate forcing is not known to better than about ±50%. All models, no matter how complicated, have adjustable parameters that are used to fit the climate data we have in our hands. Different models use different parameterizations to do this fitting. Yet when the different models are advanced into the next century, their solutions for changes diverge from one another alarmingly ($\sim \pm 50\%$). Aside from our lack of knowledge of the effects of human intervention (or lack thereof) in changing the radiation budget by altering CO_2 or aerosol concentrations, the problems seem to be centered on our lack of understanding of the climate feedback mechanisms, which are discussed in many parts of this book. Often the blame is placed on the lack of resolution of the numerical grids or lack of inclusion of enough physical processes. But as soon as a finer grid or more physical processes are introduced, even more parameters have to be inserted and adjusted to fit almost the same amount of data. The process of improving the models often leads to a phenomenon known by statisticians as *overfitting*, wherein there are too many adjustable parameters for the number of available uncorrelated observations. The different GCM simulation groups naturally use different parameterizations to arrive at their final candidate model to be entered in the beauty contest. There is a multiplicity of ways to achieve a better goodness of fit. Different groups achieve their best results in different ways. It is an oversimplification

to say the whole problem lies in the phenomenological coefficients. For example, there is freedom to choose exactly which and how many physical processes to include (or remove) to achieve a better match with available data. When conditions change into the future, the solutions diverge from one another. The great economist John Maynard Keynes once said something to the effect that "it is better to have a rough idea of the truth than a very precise estimate of an untruth." Another sage (C. E. Leith, a pioneer in climate modeling and theory) once said something to the effect of "1.1 or 1.0?" "Nonsense, this is climate science, they are equal to one another." It is not an excuse to delay action. As in medical research, decisions have to be made based on incomplete data sets (sampling errors). We press on sometimes a bit too hurriedly, but the process is surely self-correcting over time.

A final caution about EBMs. EBMs appear to work for the surface-temperature field. Some simple versions can be applied for a layered atmosphere or ocean, but the real value is at the surface where the radiation budget and pretty simple statistical and thermodynamical considerations dominate. As the focus lifts above the surface (or boundary layer), a host of new mechanisms are invoked. For example, at the surface, the response to a stimulating heating imbalance decays away in space a finite distance from the source. But above the boundary layer, such a disturbance can result in changes of local buoyancy and wavelike anomalies in density will radiate away from the source. We have been removed from the EBM world. We end these introductory remarks by cautioning the reader that our simple models are always highly idealized and might be best thought of as *analogs* to the climate system. "They are to be taken seriously, but not literally."[10]

Notes on Further Reading

Excellent descriptions of the climate system can be found in such books as Hartmann (2016) and Neelin (2011). The stratosphere and above are described in Andrews *et al.* (1987). Elementary accounts of the oceans are given in Picard and Emery (1990). The role of the Sun in the Earth's climate is nicely described at a beginners level in the book by Haigh and Cargill (2015). The articles in the volume edited by Archer and Pierrehumbert (2010) provide further historical material.

Exercises

1.1 Compute the emitted radiation of a black body whose temperature is 300 K in $W\,m^{-2}$. What is the total emitted radiation for a spherical black body the size of the Earth (radius 6000 km)?

1.2 Compute the same based on the graph in Figure 1.11.

1.3 In Figure 1.10, the energy rates are balanced at the top of the atmosphere. Show that a similar balance occurs at the surface.

10 This statement was made to GRN by the late Stephen Schneider in the 1980s.

1.4 Find the heat capacity at constant pressure for a column of air at sea level. Take the air pressure to be 10^5 Pa, leading to a mass of $P/g \approx 10^4$ kg. Now use the specific heat of dry air ($\approx 1000\,\mathrm{J\,kg^{-1}\,K^{-1}}$). Finally, if the whole column of air responds "rigidly" (i.e., the change is independent of altitude). Using the value of the radiation damping coefficient B, compute the relaxation time in days (and months) for this case. Would it be reasonable to use a mass less than that of the whole column for the diurnal cycle or the seasonal cycle?

1.5 Using the same approach as in the previous problem, compute the effective heat capacity and radiative relaxation time in months for a column of mixed layer of ocean water that has a depth of 50 m. How might this contrast in heat capacities for a square meter over land versus over ocean affect the seasonal cycle of the surface temperature field?

1.6 A certain random process has an autocorrelation function, $\rho(\tau) = \mathrm{e}^{-a\tau}$. What is the autocorrelation time of this process? How does your answer compare with the so-called e-folding scale of the autocorrelation function, that is, $a\tau_{\text{e-folding}} = 1$?

1.7 A very simple climate model is defined by the energy balance

$$C\frac{\mathrm{d}T(t)}{\mathrm{d}t} = -BT(t),$$

where C and B are constants, t is time, and $T(t)$ is the temperature departure from equilibrium. Find the time-dependent solution for a given initial condition, $T(0) = T_0$.

1.8 In the presence of some noise, the simple climate model in Problem 1.7 can be written as

$$C\frac{\mathrm{d}T(t)}{\mathrm{d}t} + BT(t) = f(t),$$

where $f(t)$ is assumed to be a normally distributed white noise time series with mean zero and variance σ^2. Write the equation above as an AR1 process, that is,

$$T_n = \lambda T_{n-1} + \gamma Z_{n-1}, \quad T_n = T(n\Delta t), \quad Z_n \sim N(0,1)$$

by determining the coefficients λ and γ.

1.9 Let $X_i \sim N(\mu, \sigma^2), i = 1, 2, \ldots, N$, be random variables with an identical normal distribution with mean μ and variance σ^2. Show that $Y = (X_1 + X_2 + \cdots + X_N)/N$ has a normal distribution with mean μ and standard deviation $\sigma/\sqrt{N}$.

1.10 According to Planck's law, radiation is determined by

$$B_\nu(T) = \frac{2h\nu^3}{c^2(\mathrm{e}^{h\nu/kT} - 1)}, \quad \nu = c/\lambda,$$

where λ is wavelength, ν is frequency, and the constant values are defined by

$h = 6.626 \times 10^{-34}$ J s : Planck's constant,
$k = 1.381 \times 10^{-23}$ J K^{-1} : Boltzmann's constant,
$c = 2.990 \times 10^{8}$ m s^{-1} : speed of light.

(The program "planck.f" can be found at the authors' (KYK) website.)

(a) Compute the radiation function for the wavelength range of (0, 2.0 μm) using temperature, 5770, 6000, and 7000 K. Plot the radiation functions in one plot.
(b) According to Wien's law, the wavelength at which the maximum radiation is reached is given by

$$\lambda_{max} T = \text{const.}$$

This constant is approximately 2900. Plot, the location of maximum radiation for the four temperature in part (a).

1.11 For this exercise, use the following files: t2m.data (2 m air temperature), insol.data (solar irradiance at TOA), nswt.data (net shortwave radiation at TOA), nsws.data (net shortwave radiation at surface), nlwt.data (net longwave radiation at TOA), and nlws.data (net longwave radiation at surface). These are the global averaged values for the period 1979–2015 (total of 813 points) derived from the NCEP/NCAR reanalysis product. (These files can be found at the author's (KYK) website.)

(a) Calculate the average albedo of the Earth.
(b) How much of the solar irradiance reaches the surface?
(c) What is the linear relationship between 2 m air temperature and net longwave radiation at the top of atmosphere (TOA)?
(d) What is the linear relationship between 2 m air temperature and net longwave radiation at the surface? Explain your result.
(e) How does the mean magnitude of net longwave radiation at TOA compare with the mean magnitude of net shortwave radiation at TOA? How do you interpret the result?